Journal of Membrane Science & Research

journal homepage: www.msrjournal.com

Research Paper

Gas Permselectivity of Hyperbranched Polybenzoxazole – Silica Hybrid Membranes Treated at Different Thermal Protocols

Tomoyuki Suzuki *, Azumi Saito

Faculty of Materials Science and Engineering, Kyoto Institute of Technology, Matsugasaki, Sakyo-ku, Kyoto 606-8585, Japan

Article info

Received 2021-07-14
Revised 2021-09-03
Accepted 2021-09-29
Available online 2021-09-29

Keywords

Hyperbranched polybenzoxazole
Silica
Sol-gel
Gas separation membrane

Highlights

- Thermally-treated hyperbranched PBO – silica hybrids for gas separation.
- Gas permeability was improved with increasing treated temperature and silica content.
- The thermally-treated hybrid membranes showed an attractive CO_2/CH_4 permselectivity.

Graphical abstract

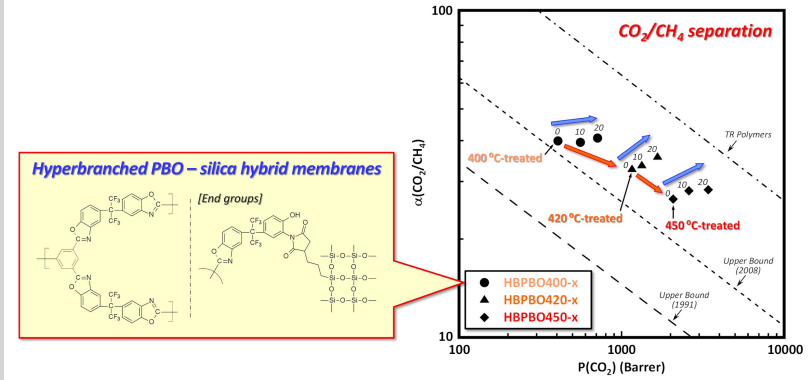

Abstract

Hyperbranched polybenzoxazole (HBPBO) – silica hybrids were treated at different thermal protocols and their gas permselectivity were studied. Inter-chain distance and free volume of pristine HBPBO were enlarged with increasing treated temperature. Gas permeability and diffusivity of the HBPBO were considerably increased with increasing treated temperature, which was resulted from increased fractional free volume due to enlarged inter-chain distance. Gas permeability of the HBPBO was further increased by the hybridization with silica, mainly owing to the increased gas diffusivity. This fact indicated additional free volume holes were formed at the HBPBO matrix – silica interfaces. It was worth noting the HBPBO – silica hybrids had a prominent CO_2/CH_4 permselectivity which exceeded the upper bound, and the CO_2/CH_4 permselectivity was enhanced with increasing treated temperature. The notable CO_2/CH_4 permselectivity of the HBPBO – silica hybrids would be achieved by the synergistic effect of characteristic hyperbranched molecular structure, thermal treatment, and hybridization with silica.

1. Introduction

Gas separation technologies such as purification of hydrocarbon gases, hydrogen production, and carbon dioxide capture and storage have been widely researched and developed to solve environmental and energy resource problems. While well-known, widespread gas separation processes including cryogenic distillation and pressure swing adsorption are currently available, they generally have some disadvantages such as restriction on the scale of equipment, high capital investment, and running cost [1,2]. In order to overcome these drawbacks, gas separation by polymeric membranes has been attracting attention as an alternative method [3,4]. One of the fundamental requirements, the polymeric membranes must possess not only high permeability but also high selectivity in a small membrane area. In our previous study about the development of novel gas separation membranes, it has been found that hyperbranched polybenzoxazole (HBPBO) and its silica hybrid membranes have a notable gas permselectivity by the synergistic effect of characteristic hyperbranched molecular structure and hybridization with silica, compared with linear polybenzoxazole (PBO) – silica hybrids with a similar molecular structure [5]. In addition, several linear PBOs and their silica hybrids have shown enhanced gas permselectivity with increasing thermal treatment temperature, resulted from increased fractional free volume due to enlarged inter-chain distance [6,7]. In the present study, effect of different thermal treatment protocols on gas permselectivity of the HBPBO – silica hybrids is investigated with the aim of further improvement of gas permselectivity. By the synergistic effect of characteristic hyperbranched molecular structure, hybridization with silica, and thermal treatment, it is expected to achieve highly enhanced gas permselectivity for the HBPBO – silica hybrids.

* Corresponding author: suzuki@kit.ac.jp (T. Suzuki)

DOI: 10.22079/JMSR.2021.533699.1478

2. Experimental

2.1. Polymerization

Hyperbranched poly(*o*-hydroxy amide) (HBPHA) as a precursor polymer was polymerized with 2,2-bis(3-amino-4-hydroxyphenyl)hexafluoropropane (6FAHP) (Tokyo Chemical Industry Co., Ltd., Japan) and 1,3,5-benzenetricarbonyl trichloride (BTC) (Sigma-Aldrich, Japan) in *N*,*N*-dimethylethanamide (DMAc) (Nacalai Tesque, Inc., Japan) as a solvent by applying the *in-situ* silylation method [8]. Detailed polymerization procedure was described elsewhere [5].

2.2. Membrane preparation

The synthesized HBPHA was dissolved in DMAc, and [(3-triethoxysilyl)propyl]succinic anhydride (TEOSPSA) (Tokyo Chemical Industry Co., Ltd., Japan) was added with stirring. Next, suitable amounts of tetraethoxysilane (TEOS) (Tokyo Chemical Industry Co., Ltd., Japan) and distilled water were added together with a catalytic amount of 1N of hydrochloric acid (Nacalai Tesque, Inc., Japan), followed by stirring overnight. Table 1 lists the compositions of the prepared reaction mixtures. Each mixture was cast on a polyester substrate and allowed to be held in a heating oven at 85 ºC for 1 hour. The prepared thin membrane was delaminated from a polyester substrate, and was fixed between metal frames with square windows. After that, the fixed membrane was dehydro-cyclized and hybridized in a heating oven under N_2 atmosphere according to the following stepwise heating protocol: (1) 100 ºC for 1 hour, (2) 200 ºC for 1 hour, and, at the last, (3) a specified temperature of 400, 420, or 450 ºC for 1 hour. As a result, HBPBO – silica (SiO_2) hybrid membranes, HBPBOz-x (z and x represents final treatment temperature (ºC) and silica content (wt%), respectively), were obtained. Schematic representation of the structure of the HBPBOz-x is shown in Figure 1.

2.3. Measuring methods

Wide-angle X-ray diffraction (WAXD), density, and thermogravimetric (TG) experiments for fundamental membrane characterization were carried out on the basis of the reported conditions, respectively [6,7]. Single gas permeation measurements were carried out at 76 cmHg and 25 ºC by the differential pressure method (permeant gases; O_2, N_2, CO_2, and CH_4) [9]. The gas permeability coefficient, *P* (Barrer), was discussed based on the solution – diffusion mechanism [10];

$$P = D \times S \quad (1)$$

where *D* (cm^2/s) and *S* (cm^3(STP) / $cm^3_{polym.}$ cmHg) are the diffusion and the solubility coefficients, respectively. Here the *D* was evaluated as follows [11];

$$D = \frac{L^2}{6t} \quad (2)$$

where *L* (cm) is the thickness of the membrane and *t* (s) denotes the time-lag during the permeation process.

3. Results and discussion

3.1. Characterizatioin of HBPBOz-xs

WAXD patterns of pristine HBPBOz-0s obtained by the different thermal protocols are shown in Figure 2. As shown in Figure 2, broad, amorphous halos with a bimodal distribution are observed, which indicates that the prepared membranes are amorphous, and would have a bottle-necked distribution of inter-chain distances [12]. The diffraction angles of the HBPBOz-0s are listed in Table 2, and the mean inter-chain distances, that is, the *d*-spacing values are calculated based on the Bragg's equation [13] (Table 2) ;

$$\lambda = 2d \sin\theta \quad (3)$$

where λ (= 1.54 Å) is the X-ray wavelength, *d* (Å) is the *d*-spacing, and θ (°) is the diffraction angle. It is pointed out the primary diffraction of the HBPBOz-0s shifts towards the smaller diffraction angle, which means the enlarged *d*-spacing, with increasing treated temperature. In addition, from the density measurements, fractional free volumes (FFVs) of the HBPBOz-0s are determined by the group contribution method [14,15], and the obtained FFVs are represented in Table 2. It can be pointed out that as the treated temperature increases, the FFV increases as similar as the *d*-spacing. This fact means increased treated temperature facilitates the enlargement of inter-chain distance, which brings about the increased free volume. From the TG measurements under airflow, thermal decomposition temperature, T_d^5, and silica content evaluated from the residual at 800 ºC are determined (Table 3). The T_d^5 of the HBPBOz-xs increases as the silica content increases. This fact means thermal stability of the HBPBOz-xs is improved by the hybridization with silica. It also turns out the proper amount of silica is contained in the prepared HBPBOz-xs.

Table 1
Composition of reaction mixtures.

Required silica content (wt.%)	Polymer (g)	DMAc (ml)	TEOSPSA (g)	TEOS (g)	H_2O (g)
0				–	–
10	0.5	5	0.050	0.212	0.110
20				0.477	0.248

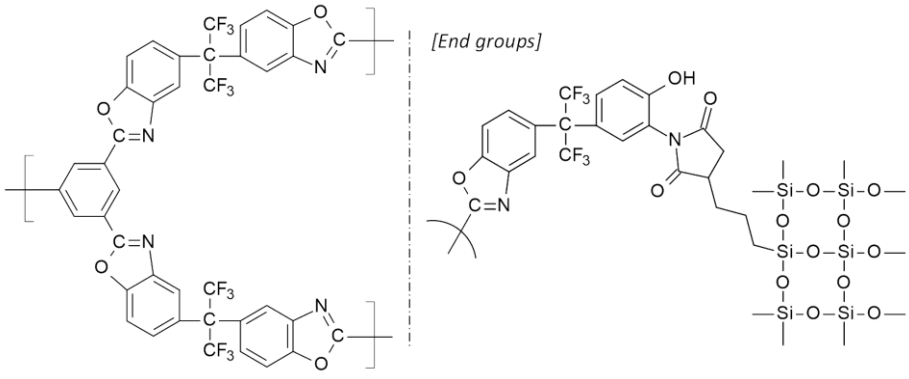

Fig. 1. Schematic representation of the HBPBOz-x.

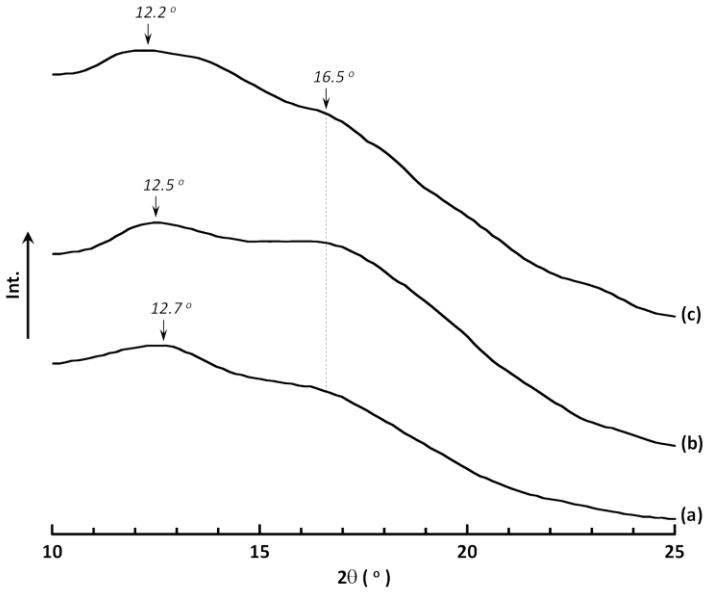

Fig. 2. WAXD patterns of HBPBO400-0 (a), HBPBO420-0 (b), and HBPBO450-0 (c).

Table 2
d-Spacing and FFV values of HBPBOz-0s

Sample	2θ (°)	*d*-spacing (Å)	Density (g/cm^3)	FFV	Ref.
HBPBO400-0	12.7, 16.5	6.96, 5.37	1.46	0.193	[5] *
HBPBO420-0	12.5, 16.5	7.07, 5.37	1.45	0.197	
HBPBO450-0	12.2, 16.5	7.25, 5.37	1.43	0.210	

* [5] contains the density and FFV values.

Table 3
Thermal properties of HBPBOz-xs.

Sample	T_d^5 (°C) *	Silica content (wt.%)
HBPBO400-0	488	0
HBPBO400-10	491	13
HBPBO400-20	502	20
HBPBO420-0	495	0
HBPBO420-10	500	10
HBPBO420-20	504	19
HBPBO450-0	498	0
HBPBO450-10	501	12
HBPBO450-20	506	21

* 5wt% weight-loss temperature under airflow.

3.2. Gas permselectivity of HBPBOz-xs

Table 4 summarizes permeability, diffusion, and solubility coefficients of the HBPBOz-xs. It can be pointed out from the comparison of the pristine HBPBOz-0s gas permeability of the HBPBOz-0s is highly increased with increasing treated temperature, and the increased permeability mainly results from the increased diffusivity. For example, the CO_2 permeability coefficient ($P(CO_2)$) of HBPBO450-0 is about 5 times higher than that of HBPBO400-0 reported previously [5]. As represented in Table 2, the increased permeability and diffusivity can be attributed to enlarged *d*-spacing and increased FFV. Focusing on the effect of the hybridization with silica, the permeability of HBPBOz-xs is increased as the silica content is increased, which is mainly attributed to the increased diffusivity. Similar phenomena have been demonstrated the addition of inorganic fillers into glassy polymers results in

highly increased permeability and diffusivity by the free volume holes additionally formed at polymer – inorganic filler interfaces [16,17]. Therefore, the increases in permeability and diffusivity of the HBPBOz-xs would result from the free volume holes formed at the HBPBO matrix – silica interfaces.

Gas separation ability in the combination of components A and B for the polymeric membranes is defined as follows [18];

$$\alpha(A/B)=\frac{P(A)}{P(B)}=\frac{D(A)}{D(B)}\times\frac{S(A)}{S(B)}=\alpha^{D}(A/B)\times\alpha^{S}(A/B) \quad (4)$$

where $\alpha(A/B)$, $\alpha^{D}(A/B)$, and $\alpha^{S}(A/B)$ represents the ideal, the diffusivity, and the solubility selectivities, respectively. Table 5 lists the separation abilities of the HBPBOz-xs in the combinations of O_2/N_2 and CO_2/CH_4. It can be pointed out the $\alpha(O_2/N_2)$ and $\alpha(CO_2/CH_4)$ essentially depend on the corresponding diffusivity selectivities, following the ordinary trend of glassy polymers [18]. Figure 3 shows the O_2/N_2 permselectivity of the HBPBOz-xs. Although the $\alpha(O_2/N_2)$ slightly decreases with increasing $P(O_2)$, it can be confirmed the HBPBOz-xs have a good O_2/N_2 permselectivity which is almost equivalent to the upper bound in 1991 [19]. It should be mentioned as shown in Figure 4 that all of the HBPBOz-xs possess significant $\alpha(CO_2/CH_4)$ values beyond the upper bound in 2008 [19], and initial $\alpha(CO_2/CH_4)$ values for each HBPBOz-0s are maintained against increased $P(CO_2)$. Considering the kinetic diameters of CO_2 (3.3 Å), O_2 (3.46 Å), N_2 (3.64 Å), and CH_4 (3.87 Å) [18], and that the CO_2/CH_4 permselectivity is essentially dominated by the diffusivity selectivity, the enhanced CO_2/CH_4 permselectivity by the hybridization with silica would be achieved by the free volume holes formed at the HBPBO matrix – silica interfaces which possess a molecular-sieving ability favorable for the CO_2/CH_4 separation. Moreover, as given in Figure 4, compared to the PBO obtained by the thermal rearrangement (TR) of the poly(*ortho*-hydroxy imide), that is consisted of 4,4'-(hexafluoroisopropylidene)diphthalic anhydride (6FDA) and 6FAHP, and its silica hybrids (TR450-x, x represents silica content (wt%)) [20], the HBPBO450-x shows a prominent CO_2/CH_4 permselectivity with higher $P(CO_2)$ than the TR450-x. The notable CO_2/CH_4 permselectivity of the HBPBO450-x would be achieved by the synergistic effect of characteristic hyperbranched molecular structure, thermal treatment, and hybridization with silica. Although the HBPBOz-xs, at present, cannot exceed the extended upper bound for TR-polymers (Figure 4) [19,21,22], the HBPBOz-xs potentially have an attractive CO_2/CH_4 permselectivity comparable to the TR-polymers.

Table 4
Permeability, diffusion, and solubility coefficients of HBPBOz-xs.

Sample	P (Barrer) *				D × 10^8 (cm^2 / s)				S × 10^2 (cm^3(STP) / $cm^3_{polym.}$cmHg)				Ref.
	CO_2	O_2	N_2	CH_4	CO_2	O_2	N_2	CH_4	CO_2	O_2	N_2	CH_4	
HBPBO400-0	407	69	17	10	8.5	23	6.5	1.1	48	3.0	2.6	8.9	[5]
HBPBO400-10	558	90	22	14	9.6	26	7.7	1.3	58	3.5	2.9	11	[5]
HBPBO400-20	713	112	27	17	14	33	9.9	1.9	51	3.3	2.8	9.2	[5]
HBPBO420-0	1161	196	51	35	20	36	12	2.5	59	5.4	4.2	14	
HBPBO420-10	1333	209	57	39	23	37	15	3.4	59	5.7	3.8	12	
HBPBO420-20	1667	240	63	46	25	50	20	4.3	66	4.8	3.1	11	
HBPBO450-0	2079	335	97	79	37	79	26	5.8	56	4.2	3.8	14	
HBPBO450-10	2596	381	110	92	49	96	32	8.9	53	4.0	3.4	10	
HBPBO450-20	3416	413	127	121	65	107	39	12	52	3.9	3.3	9.8	

* 1 Barrer = 1×10^{-10} cm^3(STP) cm / cm^2 s cmHg

Table 5
CO_2/CH_4 and O_2/N_2 selectivities of HBPBOz-xs.

Sample	CO_2/CH_4 selectivity			O_2/N_2 selectivity			Ref.
	α (CO_2/CH_4)	α^{D}(CO_2/CH_4)	α^{S}(CO_2/CH_4)	α (O_2/N_2)	α^{D}(O_2/N_2)	α^{S}(O_2/N_2)	
HBPBO400-0	40	7.5	5.4	4.2	3.6	1.2	[5]
HBPBO400-10	40	7.2	5.5	4.1	3.3	1.2	[5]
HBPBO400-20	41	7.4	5.5	4.1	3.4	1.2	[5]
HBPBO420-0	33	7.8	4.2	3.8	2.9	1.3	
HBPBO420-10	34	6.6	5.1	3.7	2.4	1.5	
HBPBO420-20	36	5.9	6.1	3.8	2.5	1.5	
HBPBO450-0	27	6.4	4.1	3.5	3.1	1.1	
HBPBO450-10	28	5.5	5.1	3.5	3.0	1.2	
HBPBO450-20	28	5.3	5.4	3.3	2.8	1.2	

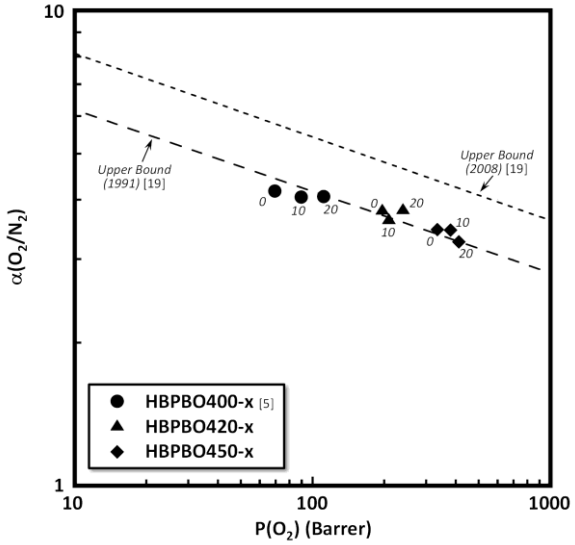

Fig. 3. O_2/N_2 permselectivity of HBPBOz-xs; the annotated number indicates the silica content in the membrane (wt.%).

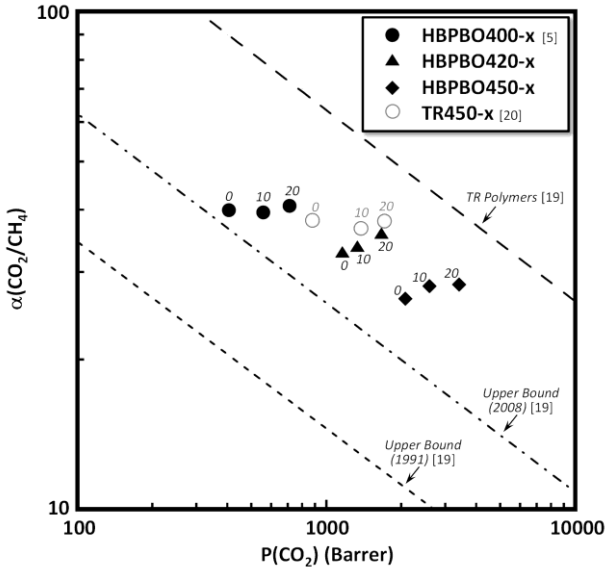

Fig. 4. CO_2/CH_4 permselectivity of HBPBOz-xs and thermally-rearranged polybenzoxazole – silica hybrids (TR450-x); the annotated number indicates the silica content in the membrane (wt.%).

4. Conclusions

Hyperbranched polybenzoxazole – silica hybrids (HBPBOz-xs) were prepared at different thermal protocols, and their gas permselectivity were studied. Gas permeability and diffusivity of the HBPBOz-xs considerably increase with increasing treated temperature, which is resulted from enlarged *d*-spacing and increased FFV. The gas permeability of the HBPBOz-xs is further increased by the hybridization with silica, mainly owing to the increased gas diffusivity. This fact suggests additional free volume holes are formed at HBPBO matrix – silica interfaces. It is worth noting the HBPBOz-xs possess a prominent CO_2/CH_4 permselectivity beyond the upper bound, and the CO_2/CH_4 permselectivity is enhanced with increasing treated temperature. The notable CO_2/CH_4 permselectivity of the HBPBOz-xs would be achieved by the free volume holes formed at the HBPBO matrix – silica interfaces that possess a molecular-sieving ability suitable for the CO_2/CH_4 separation. By the synergistic effect of characteristic hyperbranched molecular structure, thermal treatment, and hybridization with silica, the HBPBOz-xs show an attractive CO_2/CH_4 permselectivity.

Acknowledgements

This study was supported by JSPS KAKENHI Grant Number JP17K05994.

References

[1] P. Bernardo, E. Drioli, G. Golemme, Membrane gas separation: A review/state of the art, Ind. Eng. Chem. Res. 48 (2009) 4638–4663. https://doi.org/10.1021/ie8019032.

[2] D. F. Sanders, Z. P. Smith, R. Guo, L. M. Robeson, J. E. McGrath, D. R. Paul, B. D. Freeman, Energy-efficient polymeric gas separation membranes for a sustainable future: A review, Polymer 54 (2013) 4729–4761. http://dx.doi.org/10.1016/j.polymer.2013.05.075.

[3] M. L. Jue, R. P. Lively, Targeted gas separations through polymer membrane functionalization, React. Funct. Polym. 86 (2015) 88–110. http://dx.doi.org/10.1016/j.reactfunctpolym.2014.09.002.

[4] C. Z. Liang, T. S. Chung, J. Y. Lai, A review of polymeric composite membranes for gas separation and energy production, Prog. Polym. Sci. 97 (2019) 101141. https://doi.org/10.1016/j.progpolymsci.2019.06.001.

[5] T. Suzuki, M. Takenaka, Y. Yamada, Synthesis and gas transport properties of hyperbranched polybenzoxazole – silica hybrid membranes, J. Membr. Sci. 521(2017)10–17. https://doi.org/10.1016/j.memsci.2016.08.051.

[6] T. Suzuki, Y. Otsuki, Gas transport properties of polybenzoxazole–silica hybrid membranes prepared with different alkoxysilanes, Polym. J. 50 (2018) 177–186. https://doi.org/10.1038/s41428-017-0006-6.

[7] T. Suzuki, A. Saito, Preparation of polybenzoxazole–silica hybrid membranes for CO2/CH4 separation, Polym. J. 51 (2019) 1037–1044. https://doi.org/10.1038/s41428-019-0218-z.

[8] Y. Oishi, A. Konno, J. Oravec, K. Mori, Synthesis and properties of fluorine-containing polybenzoxazoles by in situ silylation method, J. Photopolym. Sci. Technol. 19 (2006) 669–672. https://doi.org/10.2494/photopolymer.19.669.

[9] S. Miyata, S. Sato, K. Nagai, T. Nakagawa, K. Kudo, Relationship between gas transport properties and fractional free volume determined from dielectric constant in polyimide films containing the hexafluoroisopropylidene group, J. Appl. Polym. Sci. 107 (2008) 3933–3944. https://doi.org/10.1002/app.27496.

[10] N. Muruganandam, W. J. Koros, D. R. Paul, Gas sorption and transport in substituted polycarbonates, J. Polym. Sci. B Polym. Phys. 25 (1987) 1999 –2026. https://doi.org/10.1002/polb.1987.090250917.

[11] D. H. Weinkauf, H. D. Kim, D. R. Paul, Gas transport properties of liquid crystalline poly(p-phenyleneterephthalamide), Macromolecules 25 (1992) 788–796. https://doi.org/10.1021/ma00028a044.

[12] C. H. Park, E. Tocci, S. Kim, A. Kumar, Y. M. Lee, E. Drioli, A Simulation study on OH-containing polyimide (HPI) and thermally rearranged polybenzoxazoles (TR-PBO): Relationship between gas transport properties and free volume morphology, J. Phys. Chem. B 118 (2014) 2746 –2757. https://doi.org/10.1021/jp411612g.

[13] H. Wang, T. S. Chung, The evolution of physicochemical and gas transport properties of thermally rearranged polyhydroxyamide (PHA), J. Membr. Sci. 385-386 (2011) 86–95. https://doi.org/10.1016/j.memsci.2011.09.023.

[14] D. W. van Krevelen, Properties of Polymers, third ed., Elsevier, Amsterdam, 1990.

[15] J. Y. Park, D. R. Paul, Correlation and prediction of gas permeability in glassy polymer membrane materials via a modified free volume based group contribution method, J. Membr. Sci. 125 (1997) 23–39. https://doi.org/10.1016/S0376-7388(96)00061-0.

[16] T. C. Merkel, B. D. Freeman, R. J. Spontak, Z. He, I. Pinnau, P. Meakin, A. J. Hill, Ultrapermeable, reverse-selective nanocomposite membranes, Science 296 (2002) 519−522. https://doi.org/10.1126/science.1069580.

[17] Y. Kudo, H. Mikami, M. Tanaka, T. Isaji, K. Odaka, M. Yamato, H. Kawakami, Mixed matrix membranes comprising a polymer of intrinsic microporosity loaded with surface-modified non-porous pearl-necklace nanoparticles, J. Membr. Sci. 597 (2020) 117627. https://doi.org/10.1016/j.memsci.2019.117627.

[18] B. D. Freeman, Basis of permeability/selectivity tradeoff relations in polymeric gas separation membranes, Macromolecules 32 (1999) 375–380. https://doi.org/10.1021/ma9814548.

[19] L. M. Robeson, The upper bound revisited, J. Membr. Sci. 320 (2008) 390–400. https://doi.org/10.1016/j.memsci.2008.04.030.

[20] T. Suzuki, Gas transport properties of thermally rearranged (TR) polybenzoxazole – silica hybrid membranes, Polymer, 214 (2021) 123274. https://doi.org/10.1016/j.polymer.2020.123274.

[21] S. H. Han, N. Misdan, S. Kim, C. M. Doherty, A. J. Hill, Y. M. Lee, Thermally rearranged (TR) polybenzoxazole: Effects of diverse imidization routes on physical properties and gas transport behaviors, Macromolecules 43 (2010) 7657–7667. https://doi.org/10.1021/ma101549z.

[22] S. Kim, Y. M. Lee, Rigid and microporous polymers for gas separation membranes, Prog. Polym. Sci. 43 (2015) 1–32. http://dx.doi.org/10.1016/j.progpolymsci.2014.10.005